Pulsatile Right Ventricle to Pulmonary Artery Extracorporeal Membrane Oxygenation in a Pigs
Running title: Pulsatile RV-PA ECMO in a piglet model

Hideshi ITOH[1, 2, 6], Shingo Ichiba[2], Hideaki Obata[3], Midori Futami[5], Shigeyuki Okahara[5], Teruyuki Kawabata[3], Nguyen The Binh[6, 7], Le Ngoc Thanh[6]*

DECLARATIONS

Funding: This study was supported by "JSPS KAKENNHI Grant Number JP19K09407".

Acknowledgments: The authors thank the graduate students in the department of biomedical engineering at the Okayama University of Science for preparing and assisting during the experimental procedures, as well as the perfusionists in the department of clinical engineering at the Okayama University Hospital for technical assistance. The authors would also like to thank all their colleagues who helped with this study.

Declaration of Conflicting interests: The authors declare that there is no conflict of interest.

Ethical Approval: The Animal Care and Use Committee of the Okayama University of Science (Okayama, Japan) approved that the experimental animals (certificate number: 2021-040) were handled in accordance with Federal Law and guidelines of the "Guide for the Care and Use of Laboratory Animals, Eighth Edition" prepared by the National Institutes of Health (NIH Publication, 2011).

Informed consent: Not applicable

Total word count: **4191 words**

Reference count: **27**

ABSTRACT

Background: We investigated the impact of right ventricle to pulmonary artery extracorporeal membrane oxygenation in acute respiratory dysfunction with or without pulsatile flow.

Methods: We used bronchoalveolar lavage with intrapulmonary administration of warm saline to establish a severe acute respiratory distress syndrome model (ratio of partial pressure of oxygen in arterial blood to the fraction of inspiratory oxygen concentration ratio <200) in eight piglets (mean body weight: 8.45±1.24 kg). The piglets were categorized into the pulsatile (N=4) and non-pulsatile extracorporeal membrane oxygenation groups (N=4). We started right ventricle to pulmonary artery extracorporeal membrane oxygenation with a 60 mL/kg/min

**Corresponding Author: Prof. Hideshi ITOH*
Department of Biomedical Engineering, Nippon Bunri University Graduate School of Engineering, Oita, Japan
1727 Ichigi, Oita, 870-0397 Japan
[1] Nippon Bunri University Graduate School of Engineering, Oita, Japan
[2] Department of Intensive Care Medicine and Clinical Engineering, Tokyo Women's Medical University Hospital, Tokyo, Japan
[3] Department of Biomedical Engineering, Okayama University of Science, Okayama, Japan
[4] Department of Bioscience, Okayama University of Science, Okayama, Japan
[5] Department of Medical Engineering, Junshin Gakuen University, Fukuoka, Japan
[6] University of Medicine and Pharmacy, Vietnam National University, Hanoi, Viet-Nam
[7] Cardiovascular Center, E Hospital, Hanoi, Viet-Nam, Hanoi
Tel: 097574848 - Email: Itohs@nbu.ac.jp
Received date: *11/10/2023* ***Accepted date:*** *25/06/2024*

flow to support the animals for 6 hours. We monitored hemodynamic data and blood gas levels for assessing base excess, and performed arterial blood sampling and electrocardiogram. Interleukin-6 and endotherlin-1 concentrations in blood plasma were evaluated before and after right ventricle to pulmonary artery extracorporeal membrane oxygenation. We compared the lung wet/dry weight ratio as a measure of pulmonary edema and collected lung tissue samples for the pathologically evaluating pneumocytes before and after right ventricle to pulmonary artery extracorporeal membrane oxygenation.

Results: We maintained stable hemodynamics and extracorporeal membrane oxygenation flow above an arterial oxygen saturation of 85% in both groups. Pneumocyte evaluation showed clearly less pulmonary edema, pulmonary fibrosis, and inflammation. Interleukin-6 concentration was less in the pulsatile group than in the non-pulsatile group.

Conclusions: Pulsatile right ventricle to pulmonary artery extracorporeal membrane oxygenation was less vasoconstrictive and maintained more effective oxygenated pulmonary flow. It ameliorates pulmonary circulation and facilitates recovery from acute respiratory failure.

Keywords: *Extracorporeal Membrane Oxygenation (ECMO), Acute Respiratory Distress Syndrome (ARDS), Right Ventricle to Pulmonary Artery (RV-PA), Pulsatile, Non-pulsatile.*

INTRODUCTION

Extracorporeal membrane oxygenation (ECMO) is a rescue modality for several etiologies of reversible cardiopulmonary failure in both children and adults, including acute respiratory distress syndrome (ARDS), acute cardiac failure, and trauma, as a bridge to lung or heart transplant (1, 2). It has been upgraded remarkably in recent years. The H1N1 influenza pandemic occurred in 2009, during which, ECMO showed favorable results in such patients with ARDS (3). In 2019, an outbreak of pneumonia caused by severe acute respiratory syndrome coronavirus 2 occurred, during which too, ECMO was used as a rescue therapy (4). Generally, veno-arterial ECMO, which drains venous blood and returns oxygenated blood to the arterial site, is used for cardiac ECMO to support the systemic circulation and supply oxygenated blood. In contrast, veno-venous ECMO (VV ECMO), which provides gas exchange but cannot provide cardiac support, drains venous blood and returns oxygenated blood to the venous site. The blood return site is usually the right atrium, pulmonary arteries, or internal jugular vein. A concern in the use of VV ECMO is that recirculation occurs when returned blood is withdrawn through the access cannula rather than flowing forward through the pulmonary circulation (5, 6). Currently, the golden standard of the ECMO circuit consists of a polymethylpentene membrane oxygenator and non-pulsatile centrifugal pump (7). Its disadvantage is that peripheral tissue perfusion is low; therefore, a higher pump flow output of 20-30% is required to match the bioavailability of a pulsatile pump (8). Additionally, tissue oxygenation and exchangeability with the membrane oxygenator are less effective than with a pulsatile pump. Pulsatile ECMO has been

shown to improve microcirculation and increase hemodynamic energy in an acute cardiac failure model. However, the effect of pulsatile VV ECMO for respiratory ECMO in ARDS recovery is unknown. In ARDS, surfactant depletion and inactivation decrease alveolar stability, exacerbating or precipitating alveolar collapse, lung atelectasis, and hypoxia. Animal models are widely used to study the pathogenic mechanisms of ARDS and the effects of interventions on clinical and biological outcomes (9). In addition, right ventricle to pulmonary artery (RV-PA) bypass is chosen to obtain a stable blood flow in VV ECMO and reduce recirculation problems. This study aimed to compare the effectiveness of pulsatile and non-pulsatile RV-PA ECMO in ARDS. To the best of our knowledge, this is the first study to evaluate the differences and similarities between pulsatile and the non-pulsatile RV-PA ECMO in a piglet model of ARDS.

MATERIALS AND METHODS

Eight piglets with a mean body weight of 8.45±1.24 kg were categorized into pulsatile (N=4) and non-pulsatile ECMO groups (N=4). The Animal Care and Use Committee of our university approved that the experimental animals (certificate number: 2021-040) were handled in accordance with Federal Law and guidelines of the "Guide for the Care and Use of Laboratory Animals, Eighth Edition" prepared by the National Institutes of Health (NIH Publication, 2011).

Experimental design

The experimental ECMO circuit (**Fig. 1**) consisted of a centrifugal pump (HPM-15; Senko Medical Instrument Mfg.co., Tokyo, Japan), membrane oxygenator (Baby-RX, Terumo, Tokyo, Japan), and in-house pneumatic pulsatile flow generator system. We used a 10 Fr ultra-thin-wall cannula (Biomedicus; Edwards Life Sciences, Irvine, CA, USA) via the pulmonary artery and a 14 Fr DLP malleable cannula (DLP; Medtronic, Minneapolis, MN, USA) via the right atrium. The circuit was primed with 250 mL acetate Ringer's solution. The pump rate was maintained at 60 beats per minute during the pulsatile RV-PA ECMO. We generated pulsatile flow using a pneumatic pulsatile flow generator system. **Figure 2** shows the pulsatile flow of the internal carotid arterial waveform and post-pneumatic pressure waveform of the pulsatile flow generator system (**Fig. 2**). Ts 410 transit-time tubing flow probes (Transonic Systems, Ithaca, NY, USA) were used to measure the flow rate in the arterial and venous lines. A cardio-press in-line pressure monitor (JMS, Tokyo, Japan) was used to measure pre- and post-pneumatic pulsatile flow generator pressures. The ECMO flow rate was set at 60 mL/kg/min as 50% of the full-support flow; animals were supported at this flow rate for 6 hours during the experiment for both pulsatile and the non-pulsatile RV-PA ECMO. We did not use any blood transfusions, inotropic drugs, or vasoactive drugs during the experiment. We monitored hemodynamic data and blood gas levels for assessing base excess, and performed arterial blood sampling and electrocardiogram. Additionally, we examined the concentrations of cytokines interleukin-6 (IL-6) and endtherlin-1 (ET-1) in the blood plasma to evaluate the inflammatory response and impact of vasoconstriction of pulmonary arteries before and after RV-PA ECMO.

Each piglet was pretreated with 10 mg midazolam and placed in the spine position on the surgical table. Anesthesia was induced with 5% sevoflurane inhalation in oxygen. The electrocardiogram electrode, return electrode

plate for electric scalpel, and pulse oximeter (Nihon Koden, Tokyo, Japan) were set at the front of the leg. A urinary catheter and rectal temperature probe were placed. The core temperature was maintained at 37.0 °C using a heated surgical table. A tracheotomy was performed and a 6 mm endotracheal tube was inserted. The endotracheal tube was connected to a respirator, and anesthesia was maintained using 5% sevoflurane with 5 to 10 L/min oxygen. The respirator was maintained at the rate of 20 times/min, with a tidal volume of 7-10 mL/kg/respiration and 100% oxygen, before starting the ECMO. An intravenous fluid route was established from the right internal jugular vein. Following the setup of the hemodynamic and ECMO monitoring equipment, 3 mg/kg of heparin sodium was administered. Anticoagulation was accomplished via drip infusion of heparin sodium to maintain an activation clotting time of 180-200 s during the experiment. In addition, an 8 Fr Foley catheter (Covidien, Tokyo, Japan) was placed in the urinary bladder to monitor urine output during the experiment. Subsequently, the pericardium was opened, and the experimental ECMO circuit was connected. We initiated non-pulsatile ECMO at the flow rate of 80 mL/kg/min for the initial 30 min of the experimental condition before simulating ARDS. Rectal temperature was maintained at 37 °C during the experiment. We weaned off ECMO at the end of the experiment (6 hours after ECMO with the initiated ARDS model). During ECMO, we collected hemodynamic data (heart rate, electrocardiogram monitoring, and internal carotid arterial blood pressure), arterial blood gas levels, arterial blood sampling data, and arterial pressure waveforms for both groups.

We used the bronchoalveolar lavage method to design the experimental piglet model of ARDS by inducing lung injury (ratio of partial pressure of oxygen in arterial blood to the fraction of inspiratory oxygen concentration [PaO_2/F_iO_2] < 200) with intrapulmonary administration of warm sodium polyacrylate (10). We compared the lung wet/dry weight ratio between the two groups as an index of lung water accumulation to diagnose pulmonary edema. Whole lungs were harvested from the experimental piglets after each procedure and weighed and dried to obtain lung wet/dry weight ratios. To measure the total amount of lung water, the experimental piglets were dissected under deep sevoflurane anesthesia, and the lung weight was measured immediately after its excision (wet weight). We dried the harvested lungs at 150 °C for 18 hours using an organ dryer (forced convention oven; DRM420DD, ADVANTEC®, Tokyo, Japan). Further, we obtained lung tissue samples for pathological evaluation of the pneumocytes using a light microscope (EVOS® XL core Imaging System, Thermo Fisher Scientific Japan, Tokyo) before and after RV-PA ECMO. The samples were excised from the dorsal-caudal regions of both lungs and fixed in 10% buffered formalin for 48 hours before sectioning. The fixed tissues were processed, embedded in paraffin, sectioned (thickness 4 um), and stained with hematoxylin-eosin. For each animal, ten randomly selected fields were assessed (original magnification ×10 and ×20, some at high magnification of ×40, and weak magnification of ×4) for alveolar fibrin deposition, alveolar inflammatory cell infiltration, and interstitial and intra-alveolar edema.

After the experiment, all animals were euthanized using an intracardiac bolus of 20 mEq/L potassium chloride (Terumo, Tokyo) under anesthesia. Death was confirmed by the

absence of cardiac electrical activity on continuous surface electrocardiography.

Blood sampling and hemodynamic profile

Approximately 200 µL of freshly sampled blood during the procedures was injected in the i-STAT System (Abbott Laboratories, Abbott park, IL, USA) with the i-STAT CG4+ (potential of hydrogen, PaO_2, and partial pressure of carbon dioxide) and CG8+ (arterial oxygen saturation, base excesses, carbonated hydrogen ion) cartridge tests. The reminder of the blood was allowed to clot at room temperature and centrifuged for the collection of serum. Serum samples were stored frozen until further analysis. Erythrocyte, thrombocyte, and leukocyte counts were determined using a fully automatic hemocytometer (Celltac alpha MEK-6450, Nihon Kohden, Tokyo, Japan). We measured concentrations of IL-6, as a biomarker associated with pro-inflammatory and anti-inflammatory responses, and, ET-1 in blood plasma or cell culture supernatants using enzyme-linked immunosorbent assay kits: Porcine IL-6 Quantikine®ELISA (R&D systems, Minneapolis, MN, USA) and Porcine ET-1 ELISA kit (Enzo life sciences Inc, New York, NY, USA). respectively.

The hemodynamic profile included measurements of the heart rate and internal carotid artery blood pressure (systolic, diastolic and mean). Data were entered via a USB port into the Labview 2009 software for Windows (Japan National Instruments, Tokyo, Japan) and collected at 20-s intervals with 1000 samples/s. We used USB-6008 (Japan National Instruments), as an analog-to-digital converter, to input flow and pressure measurement data into a personal computer for hemodynamic data analysis.

Statistical analysis

Data were analyzed using SPSS for Mac, version 28.0.1.1 (SPSS Inc., Chicago, IL, USA). All data were expressed as mean and standard deviation. The t-test and Mann-Whitney U test were used to evaluate differences between groups. A P value <0.05 was considered to indicate statistical significance. Power analyses were conducted for multivariate analysis of variance, with a significance level of 0.05 and a power of 0.6.

RESULTS

Anesthesia was maintained with 0.2 mg/hour pancuronium with Ringer's acetate solution. Time related laboratory values during the experiment were not significantly different between the pulsatile and non-pulsatile groups ($P>0.05$) (**Table 1**). Table 2 shows the hemodynamic pressure changes in the pulsatile and non-pulsatile groups. We maintained stable hemodynamics with the systolic blood pressure between 70 and 95 mmHg (**Fig. 2**), and ideal ECMO flow rate above arterial oxygen saturation of 85% in both groups (**Table 1)**. One hour after ECMO, both diastolic and mean arterial blood pressures were significantly higher in the pulsatile group ($P=0.029$, **Table 2**). The mean pulmonary artery blood pressure was significantly decreased in the pulsatile group than that in the non-pulsatile group ($P=0.029$, **Table 2**). The IL-6 concentration was significantly higher in the non-pulsatile group than in the pulsatile group after the experimental procedures ($P=0.029$) (**Table 1**). A tendency for pulmonary edema and emphysema was observed in the ARDS model before RV-PA ECMO, but the occurrence of emphysema and atelectasis had declined after pulsatile RV-PA ECMO (**Fig. 3**). We observed bleeding and congestion in the pneumocytes and inflammation

around the blood vessels after pulsatile RV-PA ECMO for 6 hours (**Fig. 3**). The analysis of pneumocytes showed less pulmonary edema and pulmonary fibrosis after both types of RV-PA ECMO (**Fig. 3**). The mean lung wet/dry weight proportion was 14.80% in the pulsatile group and 14.10% in the non-pulsatile group (**Fig. 4)**.

DISCUSSION

ECMO has been used as a powerful mechanical respiratory and circulatory support system in critical situations. It may also be effective in patients with severe reversible myocardial dysfunction or ARDS. Due to its origin, the use of ECMO is much better established in neonatal and pediatric populations (10). On the one hand, it is true that ECMO is developing and has a disadvantage that satisfactory outcomes may not be achieved clinically. According to the Extracorporeal Life Support Organization registry report, ECMO has been used in more than 192,329 cases and pulmonary ECMO in 96,582 cases in January 2023 (11). The current reported survival and subsequent discharge rate after ECMO for neonatal pulmonary failure is 72%, pediatric pulmonary failure is 61%, and adult pulmonary failure if 58% (11). ARDS is a clinically and biologically heterogenous disorder associated with several disease processes that lead to acute lung injury with increased non-hydrostatic extravascular lung water, reduced compliance, and severe hypoxemia (12). Despite significant advances in the understanding and treatment of ARDS, the mortality rate associated with ARDS remains high. Generally, ECMO is composed of mechanical pumps and maintains a continuous blood flow. Pulsatile ECMO has provided better results than non-pulsatile ECMO in acute cardiac failure in fundamental experiments. In general, VV ECMO has been used for ARDS in clinical practice (13). It is performed using two basic approaches for delivery of blood with complete gas exchange: one with two site cannulations for blood access and return and the other with single double-lumen cannulations. A well-known major drawback in the former configuration is recirculation (5, 14, 15). Recirculation leads to poor oxygenation efficiency in the pulmonary circulation and may cause hypercapnia. To resolve these issues, we established and evaluated the efficacy of RV-PA ECMO for ARDS. In this study, we compared the effects of pulsatile and non-pulsatile flow of RV-PA ECMO in an acute respiratory failure model in piglets. Our results showed that none of the two types of RV-PA ECMO, with/or without pulsatile flow, cause hypercapnia (**Table 1**). Strictly speaking, the non-pulsatile group tended to have a higher partial pressure of carbon dioxide than the pulsatile group but within the reference range. Hypoxic pulmonary vasoconstriction is a homeostatic mechanism that is intrinsic to the pulmonary vasculature. In fact, our results showed that the mean pulmonary artery blood pressure was significantly decreased in the pulsatile group (**Table 2**). This shows that pulsatile RV-PA ECMO reduced pulmonary vascular resistance to a greater extent than non-pulsatile RV-PA ECMO. Intrapulmonary arteries constricted in response to alveolar hypoxia, diverting blood to better-oxygenated lung segments, thereby optimizing ventilation/perfusion matching and systemic oxygen delivery (16). Our results show that the direct flow of RV-PA ECMO without recirculation provides better microcirculation in the pulmonary capillary beds, which can prevent hypoxic pulmonary vasoconstriction and hypercapnia.

Pathophysiologically, ARDS is diffuse alveolar damage that leads to protein-rich pulmonary edema, local alveolar hypoventilation, and atelectasis (12, 17, 18). Our results demonstrated that RV-PA ECMO with and without pulsatility improved symptoms of respiratory failure both with and without pulsatility. The evaluation of pneumocytes clearly showed less pulmonary edema, pulmonary fibrosis, and inflammation after RV-PA ECMO (**Fig. 3**). Generally, during VV ECMO, oxygenated blood from the pump is returned to the body where it is mixed with deoxygenated blood from the systemic venous return. As native lung functions improve, the systemic arterial saturation increases (15). The Extracorporeal Life Support Organization guidelines define an arterial oxygen saturation exceeding 75-80% as adequate during VV ECMO (15). Our results showed arterial oxygen saturation of more than 85% and PaO_2 of more than 55 mmHg during experimental procedures in both groups (**Table 1**). These values of oxygenation are acceptable for VV ECMO as considering the oxygen dissociation curve. In addition, hemodynamic data during procedures in both groups were stable and adequate venous drainage and perfusion flow were achieved with RV-PA ECMO. This implies that RV-PA ECMO provides better systemic arterial saturation. Further, RV-PA ECMO could lead to a resting RV heart and improve RV functions and ARDS symptoms. The lung wet/dry weight ratio was used to evaluate the severity of pulmonary edema, but it was not significantly different between the two groups (**Fig. 4**, P=0.87). Animals in both groups recovered from pulmonary edema after RV-PA ECMO. In our opinion, achievement of a resting RV heart using RV-PA ECMO with/or without pulsatility would be an advantage in pediatric procedures and patients with heart failure and respiratory failure.

Interestingly, pulsatile RV-PA ECMO led to less inflammation and achieved better ventilation. The IL-6 classic signaling is linked to anti-inflammatory functions while trans-signaling is associated with pro-inflammatory responses. IL-6 is known to regulate the synthesis of acute phase proteins, and its levels are elevated in the circulation during inflammatory conditions (19, 20). Since mechanical stress causes the release of adenosine 5'-triphosphate (ATP) by lung epithelial cells, and since ATP stimulates the release of inflammatory cytokines by cultured macrophages, dendritic cells, or both, the purinergic receptor system may be involved in the development of inflammatory reactions because of mechanical stresses in the lungs (21, 22). Generally, protein expression in endothelial cells caused by shear stress in IL-6 concentration is stimulated 24-48 hours after initiating ECMO (23). Our results demonstrate that 6 hours after initiating ECMO, IL-6 concentration was lower in the pulsatile group than in the non-pulsatile group. This means that pulsatile flow may lead to reduced inflammatory responses owing to the ability of pulsatile perfusion to sustain better in the functional state of microcirculation (8, 18, 24, 25). Pulsatile RV-PA ECMO may have led to improved respiratory function and recovery from ARDS compared to non-pulsatile RV-PA ECMO.

According to our results, there was no significant difference in ET-1 expression between the pulsatile and non-pulsatile groups. However, ET-1 expression tended to be higher in the non-pulsatile group. The reference range of ET-1 concentration is 2.0-3.0 pg/mL (26). The protein expression in endothelial cells caused by increase in ET-1 concentration is stimulated 2-24 hours

after ECMO initiation (27). Both groups exhibited higher ET-1 concentrations, although ET-1 concentration was 5-6 times more than the normal range of ET-1 in the non-pulsatile group, compared to the 2-3 times more than the normal range in pulsatile group. Hence, we believe that pulsatile flow may act to depress ET-1 expression compared to the non-pulsatile one.

The limitations of the present study are that we evaluated the effect of pulsatile RV-PA ECMO in a limited number of piglets with ARDS. A further study is required to investigate the efficacy of pulsatile flow in a chronic RV failure model and its long-term significance.

RV-PA ECMO for ARDS achieves better respiratory and cardiac functions by pumping high oxygenated blood flow to the respiratory circulation and reducing RV preloads. Especially, we found that early improvement in respiratory function can be expected with pulsatile RV-PA ECMO, caused by reduction in acute inflammatory responses owing to the ability of pulsatile perfusion to improve the pulmonary flow and sustain a functional state of microcirculation in the pulmonary capillary beds and preventing pulmonary vasoconstriction.

Based on our study, we believe that further research upon the effect of pulsatile blood flow to major organs might yield interesting results. A future in vivo study is required in a clinical setting with pulsatile ECMO including RV-PA ECMO. Such a study will provide better clinical results in both acute and chronic conditions in severe organs dysfunctions with ECMO support.

REFERENCES

1. Mosier JM, Kelsey M, Raz Y, Gunnerson KJ, Meyer R, Hypes CD, et al. Extracorporeal membrane oxygenation (ECMO) for critically ill adults in the emergency department: history, current applications, and future directions. *Crit Care* 2015; 19: 431.

2. Millar JE, Fanning JP, McDonald CI, McAuley DF, Fraser JF. The inflammatory response to extracorporeal membrane oxygenation (ECMO): a review of the pathophysiology. *Crit Care* 2016; 20: 387.

3. Australia and New Zealand Extracorporeal Membrane Oxygenation (ANZ ECMO) Influenza Investigators, Davies A, Jones D, Bailey M, Beca J, Bellomo R, et al. Extracorporeal membrane oxygenation for 2009 influenza A(H1N1) acute respiratory distress syndrome. *JAMA* 2009; 302: 1888–1895.

4. Barbaro RP, MacLaren G, Boonstra PS, Combes A, Agerstrand C, Annich G, et al. Extracorporeal membrane oxygenation for COVID-19: evolving outcomes from the international Extracorporeal Life Support Organization Registry. *Lancet* 2021; 398: 1230–1238.

5. Abrams D, Bacchetta M, Brodie D. Recirculation in venovenous extracorporeal membrane oxygenation. *ASIAO J* 2015; 61: 115–121.

6. Conrad SA, Wang D. Evaluation of recirculation during venovenous extracorporeal membrane oxygenation using computational fluid dynamics incorporating fluid-structure interaction. *ASAIO J* 2021; 67: 943–953.

7. Ündar A, Kunselman AR, Barbaro RP, Alexander P, Patel K, Thomas NJ. Centrifugal or roller blood pumps for neonatal venovenous extracorporeal membrane oxygenation: Extracorporeal Life Support Organization database comparison of mortality and morbidity. *Pediatr Crit Care Med* 2023; 24: 662–669.

8. Kim HK, Son HS, Fang YH, Park SY, Hwang CM, Sun K. The effects of pulsatile flow upon renal tissue perfusion during cardiopulmonary bypass: a comparative study of pulsatile and nonpulsatile flow. *ASAIO J* 2005; 51: 30–36.

9. Henderson WR, Barnbrook J, Dominelli PB, Griesdale DEG, Arndt T, Molgat-Seon Y, et al. Administration of intrapulmonary sodium polyacrylate to induce lung injury for the development of a porcine model of early acute

respiratory distress syndrome. Intensive Care Med Exp 2014; 2: 5.

10. Robinson S, Peek G. The role of ECMO in neonatal & paediatiric patients. *Paediatr Child Health* 2015; 25: 222–227.

11. Extracorporeal Life Support Organization Registry report. ELSO, 2020.

12. Banavasi H, Nguyen P, Osman H, Soubani AO. Management of ARDS - what works and what does not. *Am J Med Sci* 2021; 362: 13–23.

13. Al-Fares AA, Ferguson ND, Ma J, Cypel M, Keshavjee S, Fan E, et al. Achieving safe liberation during weaning from VV-ECMO in patients with severe ARDS: the role of tidal volume and inspiratory effort. *Chest* 2021; 160: 1704–1713.

14. Palmér O, Palmér K, Hultman J, Broman M. Cannula design and recirculation during venovenous extracorporeal membrane oxygenation. *ASAIO J* 2016; 62: 737–742.

15. Maratta C, Potera RM, van Leeuwen G, Castillo Moya A, Raman L, Annich GM. Extracorporeal Life Support Organization (ELSO): 2020 Pediatric Respiratory ELSO guideline. *ASAIO J* 2020; 66: 975–979.

16. Dunham-Snary KJ, Wu D, Sykes EA, Thakrar A, Parlow LRG, Mewburn JD, et al. Hypoxic pulmonary vasoconstriction: from molecular mechanisms to medicine. *Chest* 2017; 151: 181–192.

17. Cardinal-Fernández P, Lorente JA, Ballén-Barragán A, Matute-Bello G. Acute respiratory distress syndrome and diffuse alveolar damage. New insights on a complex relationship. *Ann Am Thorac Soc* 2017; 14: 844–850.

18. Gierhardt M, Pak O, Walmrath D, Seeger W, Grimminger F, Ghofrani HA, et al. Impairment of hypoxic pulmonary vasoconstriction in acute respiratory distress syndrome. *Eur Respir Rev* 2021; 30: 210059.

19. Heinrich PC, Behrmann I, Haan S, Hermanns HM, Müller-Newen G, Schaper F. Principles of interleukin (IL)-6-type cytokine signalling and its regulation. *Biochem J* 2003; 374: 1–20.

20. Ehlting C, Wolf SD, Bode JG. Acute-phase protein synthesis: a key feature of innate immune functions of the liver. *Biol Chem* 2021; 402: 1129–1145.

21. Yamamoto K, Sokabe T, Ohura N, Nakatsuka H, Kamiya A, Ando J. Endogenously released ATP mediates shear stress-induced Ca2+ influx into pulmonary artery endothelial cells. *Am J Physiol Heart Circ Physiol* 2003; 285: H793–H803.

22. Tu LN, Hsieh L, Kajimoto M, Charette K, Kibiryeva N, Forero A, et al. Shear stress associated with cardiopulmonary bypass induces expression of inflammatory cytokines and necroptosis in monocytes. *JCI Insight* 2021; 6: e141341.

23. Zegeye MM, Lindkvist M, Fälker K, Kumawat AK, Paramel G, Grenegård M, et al. Activation of the JAK/STAT3 and PI3K/AKT pathways are crucial for IL-6 trans-signaling-mediated pro-inflammatory response in human vascular endothelial cells. *Cell Commun Signal* 2018; 16: 55.

24. Li G, Zeng J, Liu Z, Zhang Y, Fan X. The pulsatile modification improves hemodynamics and attenuates inflammatory responses in extracorporeal membrane oxygenation. *J Inflamm Res* 2021; 14: 1357–1364.

25. Kanagrajan D, Heinsar S, Gandini L, Suen JY, Dau VT, Fraser JF, et al. Preclinical stdies on pulsatile veno-arterial extracorporeal membrane oxygenation: a systematic review. *ASAIO J* 2023; 69; e167-e180.

26. Kostov K, Blazhev A. Circulating levels of endothelin-1 and big endothelin-1 in patients with essential hypertension. *Pathophysiology* 2021; 28: 489–495.

Ostrow LW, Suchyna TM, Sachs F. Stretch induced endothelin-1 secretion by adult rat astrocytes involves calcium influx via stretch-activated ion channels (SACs). *Biochem Biophys Res Commun* 2011; 410: 81–86.

FIGURE LEGENDS

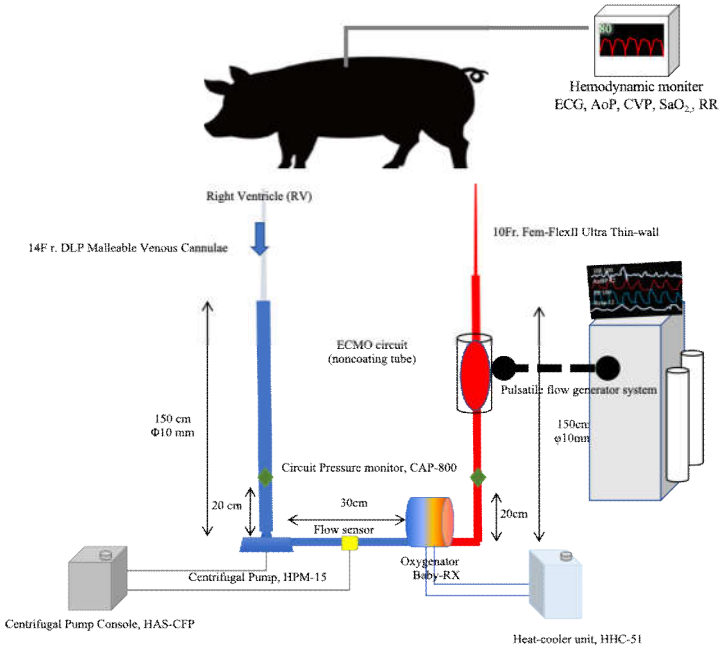

Fig. 1. Experimental RV-PA ECMO circuit

The experimental RV-PA ECMO circuit for this study consists of an HPM-15 centrifugal pump (MERA), Baby-RX (Terumo) as the membrane oxygenator, and an in-house pneumatic pulsatile flow generator system. We used a 10 Fr. Fem-Flex ultra-thin-wall cannula (Edwards Life Sciences) via the PA and a 14 Fr. DLP straight cannula (Medtronic) via the RA. The circuit was primed with 250 mL Ringer's acetate solution.

RV-PA ECMO, right ventricle to pulmonary artery extracorporeal membrane oxygenation; PA, pulmonary artery; RA, right atrium

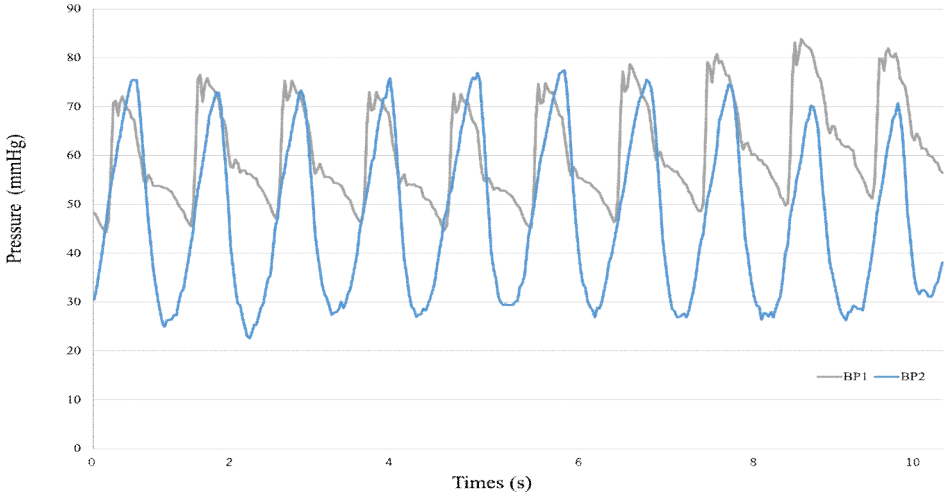

Fig. 2. Pulsatile Wave Form

Arterial pressure waveform of pulsatile flow during pulsatile RV-PA ECMO.

RV, right ventricle; PA, pulmonary artery; BP1, internal carotid artery waveform; BP2, post-pneumatic pressure waveform of the pulsatile flow generator system; RV-PA ECMO, right ventricle to pulmonary artery extracorporeal membrane oxygenation.

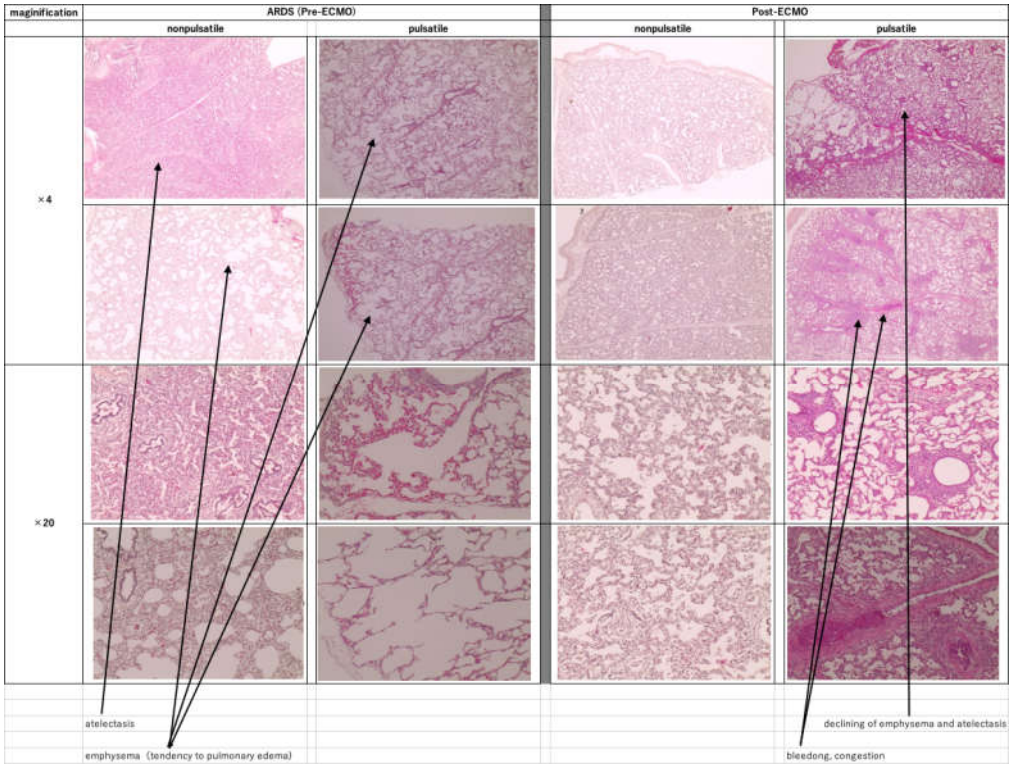

Fig. 3. Pathological evaluation for pneumocytes with a light microscope before and after the nonpulsatile and pulsatile RV-PA ECMO

RV-PA ECMO, right ventricle to pulmonary artery extracorporeal membrane oxygenation

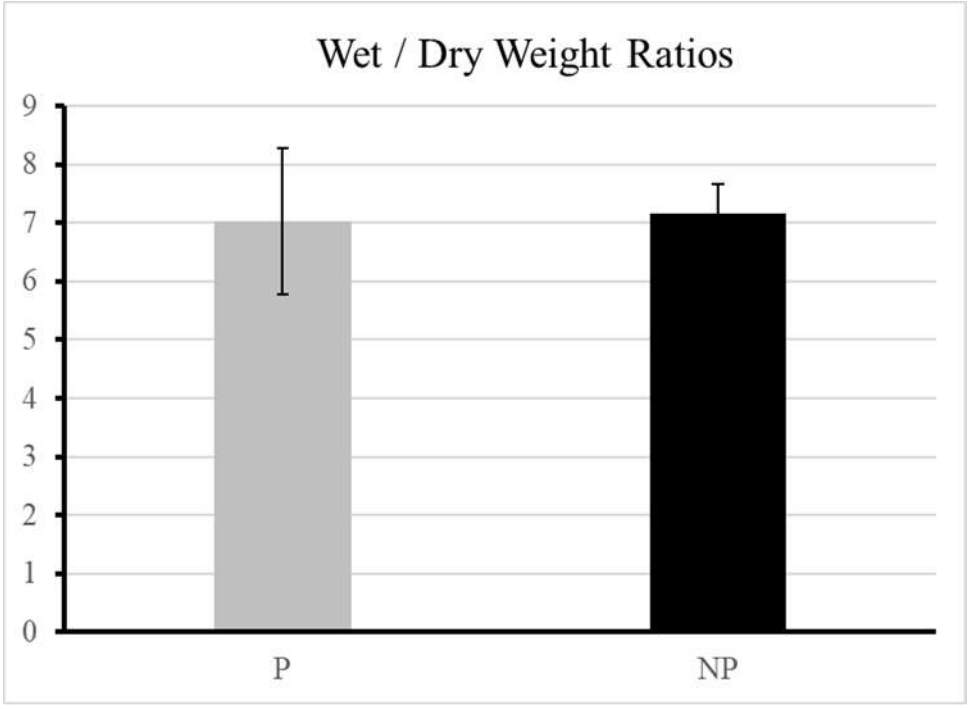

Fig. 4. The lung wet/dry weight ratios

N.S., not significant

Table 1. Time-dependent laboratory values during procedures in pulsatile and nonpulsatile groups

		After induction of anesthesia	After inductuion of ARDS model	After 1h ECMO	After 3h ECMO	After 6h ECMO
PH	P	7.64 ± 0.53	7.64 ± 0.53	7.24 ± 0.44	7.29 ± 0.27	7.18 ± 0.25
	NP	7.53 ± 0.11	7.37 ± 0.15	7.29 ± 0.02	7.20 ± 0.15	7.14 ± 0.19
PO2 (mmHg)	P	302.00 ± 33.21	60.25 ± 33.21	77.00 ± 8.45	57.75 ± 7.23	70.00 ± 5.57
	NP	308.50 ± 38.73	57.75 ± 12.66	70.25 ± 8.22	60.75 ± 12.50	61.00 ± 15.12
PCO2 (mmHg)	P	33.40 ± 3.11	37.53 ± 17.58	34.05 ± 18.50	27.28 ± 15.39	24.98 ± 10.73
	NP	32.70 ± 2.38	53.25 ± 15.18	47.18 ± 5.61	44.53 ± 8.91	44.25 ± 9.52
BE (mmol/L)	P	- 0.75 ± 5.97	2.00 ± 10.45	- 5.75 ± 3.30	- 6.00 ± 2.94	-7.25 ± 2.06
	NP	3.50 ± 1.29	4.25 ± 1.26	- 4.00 ± 1.83	- 7.00 ± 0.82	- 7.75 ± 1.71
HCO3- (mmol/L)	P	23.43 ± 4.93	24.15 ± 3.16	22.50 ± 4.47	20.05 ± 2.90	19.55 ± 3.28
	NP	33.05 ± 1.92	29.38 ± 1.03	21.65 ± 0.78	17.30 ± 1.34	20.68 ± 3.67
SaO2 (%)	P	99.25 ± 0.93	86.00 ± 7.26	92.25 ± 2.63	89.00 ± 3.37	90.50 ± 2.52
	NP	100.00 ± 0.00	90.25 ± 7.41	94.50 ± 0.58	89.00 ± 0.00	87.50 ± 4.65
Na (mmol/L)	P	141.75 ± 5.97	143.50 ± 4.36	144.75 ± 2.22	143.75 ± 2.22	145.75 ± 4.50
	NP	140.25 ± 0.96	142.25 ± 0.96	143.50 ± 1.73	145.25 ± 2.63	145.50 ± 2.65
K (mmol/L)	P	3.48 ± 1.75	3.50 ± 0.99	3.50 ± 1.31	3.65 ± 0.77	3.58 ± 0.96
	NP	4.05 ± 0.58	3.73 ± 0.22	3.65 ± 0.50	3.23 ± 0.95	3.25 ± 0.95
Ca (mmol/L)	P	1.32 ± 0.13	1.31 ± 0.04	1.28 ± 0.08	1.36 ± 0.07	1.27 ± 0.21
	NP	1.37 ± 0.07	1.32 ± 0.03	1.31 ± 0.04	1.33 ± 0.06	1.34 ± 0.08
Glu (mg/dL)	P	114.00 ± 55.54	115.25 ± 34.41	119.00 ± 42.39	134.00 ± 44.77	127.25 ± 45.46
	NP	117.5 ± 44.44	140.25 ± 15.97	153.50 ± 33.67	140.50 ± 29.94	133.75 ± 34.89
HCT (%)	P	27.75 ± 9.56	24.00 ± 2.16	21.25 ± 2.63	19.50 ± 2.65	17.50 ± 1.29
	NP	27.50 ± 5.57	23.75 ± 1.26	21.00 ± 0.82	19.75 ± 0.96	17.75 ± 2.50
Hb (g/dL)	P	9.13 ± 2.73	8.15 ± 0.74	7.40 ± 0.96	6.68 ± 1.13	5.88 ± 0.49
	NP	9.58 ± 2.30	8.00 ± 0.41	7.20 ± 0.22	6.93 ± 0.15	5.98 ± 0.87
P/F Ratio	P	302.00 ± 17.33	60.25 ± 12.45	366.67 ± 40.22	275.00 ± 34.42	316.67 ± 39.75
	NP	308.75 ± 33.54	57.75 ± 10.96	334.94 ± 33.90	288.92 ± 51.54	290.61 ± 62.36
IL-6 (pg/mL)	P	16.33 ± 5.72				21.64± 10.13
	NP	3.18 ± 1.47				283.73 ± 62.31*
ET-1 (pg/mL)	P	5.41 ± 1.66				9.83 ± 7.49
	NP	7.43 ± 0.70				16.29 ± 12.23

Power analyses were higher than 0.6 for all data.

*P<0.05, pulsatile RV-PA ECMO versus non-pulsatile RV-PA ECMO.

Glu, glucose; HCT, hematocrit; P/F ratio, PaO_2 / F_iO_2 ratio; IL-6, interleukin-6; ET-1, endtherlin-1;RV-PA ECMO, right ventricle to pulmonary artery extracorporeal membrane oxygenation

Table 2. Hemodynamic pressure changes in pulsatile and non-pulsatile groups

		After induction of anesthesia	After inductuion of ARDS model	After 1h ECMO	After 3h ECMO	After 6h ECMO
HR (BPM)	P	140.50 ± 17.40	125.25 ± 8.87	112.24 ± 14.88	109.75 ± 9.81	121.50 ± 14.37
	NP	123.00 ± 18.12	107.50 ± 21.65	130.00 ± 1.41	128.25 ± 10.91	128.50 ± 11.08
SBP (mmHg)	P	105.25 ± 22.35	104.00 ± 17.19	80.25 ± 5.89	82.25 ± 8.47	95.00 ± 5.61
	NP	120.00 ± 12.25	104.75 ± 6.98	75.25 ± 9.36	96.75 ± 13.8	92.75 ± 7.92
DBP (mmHg)	P	64.00 ± 15.92	63.50 ± 19.24	49.75 ± 5.67*	47.25 ± 9.52	56.00 ± 6.82
	NP	61.75 ± 7.69	75.00 ± 17.13	33.00 ± 2.24	48.25 ± 1.79	43.75 ± 9.18
MAP (mmol/L)	P	79.00 ± 16.90	76.50 ± 18.77	66.00 ± 5.24*	55.00 ± 5.85	72.00 ± 4.12
	NP	83.25 ± 9.58	84.50 ± 16.32	47.75 ± 2.77	64.00 ± 4.90	60.75 ± 8.58
MPAP (mmHg)	P		32.75 ± 3.11			10.7 ± 3.03*
	NP		31.25 ± 4.44			20.5 ± 3.64

Power analyses were higher than 0.6 for all data.

*P<0.05, pulsatile RV-PA ECMO versus nonpulsatile RV-PA ECMO.

HR (BPM), heart rate (beats per minutes); SBP, systolic blood pressure; DBP, diastolic blood pressure; MAP, mean arterial pressure; MPAP, mean pulmonary artery pressure; RV-PA ECMO, right ventricle to pulmonary artery extracorporeal membrane oxygenation.